Evolution of structural relaxation spectra of glycerol within the gigahertz band

T. Franosch, W. Götze,* M. R. Mayr, and A. P. Singh
Physik Department, Technische Universität München, 85747 Garching, Germany
(Received 5 August 1996)

The structural relaxation spectra and the crossover from relaxation to oscillation dynamics, as measured by Wuttke *et al.* [Phys. Rev. Lett. **72**, 3052 (1994)] for glycerol within the GHz band by depolarized light scattering, are described by the solutions of a schematic mode coupling theory model. The applicability of scaling laws for the discussion of the model solutions is considered. [S1063-651X(97)13103-8]

PACS number(s): 64.70.Pf, 61.20.Lc

I. INTRODUCTION

Traditionally the dynamics of glass-forming liquids such as glycerol was studied in a frequency window extending from, say, 0.01 Hz up to 1 MHz. One observes spectra or decay curves whose characteristic time scales τ shift drastically with changes of temperature T, and which are stretched over huge dynamical windows. The underlying processes are referred to as structural relaxation. The slowest process, which manifests itself as a characteristic low-frequency peak in susceptibility spectra, is called the α process [1]. Great progress has been made recently in extending the accessible window toward higher frequencies. For example, dielectric loss spectra of glycerol are now available up to 370 GHz [2]. The reported high frequency spectra are similar to and as puzzling as the ones measured at lower frequencies. On the other hand, normal liquids have their spectra within the THz band, and they do not exhibit structural relaxation. Thus there is the question: how do structural relaxation phenomena appear upon cooling or compression? For glycerol and other conventional glass formers the appearance must occur within the GHz window. The first complete measurements of the evolution of structural relaxation were reported by Li *et al.* [3] for the mixed salt $Ca(NO_3)_2KNO_3$ (CKN), and by van Megen and Underwood [4] for a colloid. Also for glycerol the appearance of structural relaxation spectra was studied recently [5–8] by light and neutron scattering, and in this paper quantitative interpretation of the light scattering data [6] shall be presented.

The evolution of structural relaxation is the subject of the mode-coupling theory (MCT). Originally this theory was proposed as an approximation theory for simple classical liquids [9]. It aims at the evaluation of a set of M autocorrelation functions for density fluctuations as a function of time t, $\Phi_q(t)$, $q=1,\ldots,M$, and of the corresponding susceptibility spectra $\chi_q''(\omega)$ as a function of frequency ω. $\Phi_q(t)$ obey the initial conditions $\Phi_q(0)=1$ and $\partial_t\Phi_q(0)=0$, and they are to be calculated from the closed equations of motion

$$\partial_t^2\Phi_q(t)+\Omega_q^2\Phi_q(t)+\int_0^t[M_q^{\mathrm{reg}}(t-t')+\Omega_q^2 m_q(t-t')]\partial_{t'}\Phi_q(t')dt'=0, \tag{1a}$$

$$m_q(t)=\mathcal{F}_q(\Phi(t)). \tag{1b}$$

Here $\Omega_q>0$ are M characteristic frequencies. $M_q^{\mathrm{reg}}(t)$ are M regular fluctuating force correlation functions. The numbers Ω_q and the functions $M_q^{\mathrm{reg}}(t)$ describe the transient dynamics. In a simplest approach, the regular kernel is modeled to describe a Markov process: $M_q^{\mathrm{reg}}(t)=\nu_q\delta(t)$, with $\nu_q\geqslant 0$ denoting some friction constant. The essence of the theory is Eq. (1b), which expresses the kernel m_q for a retarded friction as a polynomial $\mathcal{F}_q$ of the set of M correlators Φ. The non-negative coefficients of the mode-coupling polynomial $\mathcal{F}_q$ are given in terms of the liquid structure factors. They serve as the coupling constants of the model, and depend smoothly on control parameters like T. MCT brings out a bifurcation transition from ergodic liquid solutions to ideal glass states in the sense defined by Edwards and Anderson [10]. If the temperature is lowered, there appears a critical value T_c, so that for $T>T_c$ the solutions of Eqs. (1) exhibit relaxation of all correlators $\Phi_q(t)$ to the equilibrium value zero. For $T\leqslant T_c$ however, spontaneous arrest is obtained: $\Phi_q(t\to\infty)=f_q>0$. If T is lowered toward and through T_c, the solutions exhibit features which have a similarity to the known experimental facts for structural relaxation. For details, the reader is referred to Ref. [11]. Wuttke *et al.* [6] argued that their light scattering spectra for glycerol can be rationalized within the known MCT scenario, and one aim of this paper is to corroborate their reasoning.

For small ω and small values for the separation parameter $\sigma=C(T_c-T)/T_c$, Eqs. (1) lead to

$$\Phi_q(\omega)=\frac{-1}{\omega-1/m_q(\omega)}, \tag{2a}$$

where $\Phi_q(\omega)$ and $m_q(\omega)$ denote the Fourier-Laplace transform of $\Phi_q(t)$ and $\mathcal{F}_q(\Phi(t))$, respectively. This equation is scale invariant: with $\Phi_q(t)$, $\Phi_q^x=\Phi_q(xt)$ is also a set of solutions for all $x>0$. The slow dynamics near the bifurcation point is determined by Eq. (2a) only up to some overall time scale t_0. This dynamics is given by $\mathcal{F}_q$, i.e., by the equilibrium structure. The M frequencies Ω_q and kernels

*Also at Max-Planck-Institut für Physik (Werner-Heisenberg-Institut), P.O. Box 401212, 80805 München, Germany.

$M_q^{\mathrm{reg}}(t)$ merely determine the value for t_0 [11]. One can show that the specified slow dynamics deals with relaxation [12], i.e., the solutions can be written as a superposition of Debye laws:

$$\Phi_q(t)=\int_0^\infty e^{-\Gamma t}\varrho_q(\Gamma)d\Gamma, \quad \varrho_q(\Gamma)\geqslant 0. \tag{2b}$$

A further simplification of the mathematical problem is possible if one restricts oneself to a mesoscopic dynamical window, where $|\Phi_q(t)-f_q(T=T_c)|$ or $|\omega\Phi_q(\omega)+f_q(T=T_c)|$ are small. In a leading order $\sqrt{|\sigma|}$ expansion one arrives at a scaling law for the susceptibility spectrum,

$$\chi_A''=h_A c_\sigma \hat{\chi}_\pm(\omega t_\sigma), \quad \sigma\gtrless 0. \tag{3a}$$

Here A denotes some probing variable which couples to $\Phi(t)$; its specification enters the amplitude h_A only. In particular one can use Eq. (3a) for $\chi_q''(\omega)$, where the dependence on q merely appears in factor h_q. For the aforementioned light scattering experiments [6] the test variable A presumably is the anisotropic part of the molecule's polarizability tensor. It is straightforward to evaluate from functional $\mathcal{F}_q$ a number λ, called the exponent parameter. It determines the σ-independent master functions $\hat{\chi}_\pm$, whose quantitative details are well understood [13]. For large rescaled frequencies one obtains the critical spectrum $\hat{\chi}_\pm(\hat{\omega}\gg 1)=\sin(\pi a/2)\Gamma(1-a)\hat{\omega}^a+\mathcal{O}(\hat{\omega}^{-a})$, specified by the critical exponent a, $0<a<\frac{1}{2}$. For small $\hat{\omega}$ the glass susceptibility varies regularly $\hat{\chi}_+(\hat{\omega}\ll 1)=C_0\hat{\omega}+\mathcal{O}(\hat{\omega}^3)$. Hence there appears a knee for the $\log\hat{\chi}$ versus $\log\hat{\omega}$ diagram at some frequency $\hat{\omega}_k$ where $\hat{\chi}_+(\hat{\omega}_k)=\hat{\chi}_k$. For small rescaled frequencies the liquid spectra follow the von Schweidler law $\hat{\chi}(\hat{\omega}\ll 1)=B\ \sin(\pi b/2)\Gamma(1+b)\hat{\omega}^{-b}+\mathcal{O}(\hat{\omega}^b)$, specified by the von Schweidler exponent b, $0<b\leqslant 1$. Thus there appears a minimum at some frequency $\hat{\omega}_{\min}$, where $\hat{\chi}(\hat{\omega}_{\min})=\hat{\chi}_{\min}$. Let us reiterate that the exponents a, b, and all the constants B, C_0, $\hat{\omega}_k$, $\hat{\chi}_k$, $\hat{\omega}_{\min}$, and $\hat{\chi}_{\min}$ are given by λ, they can be taken from published tables [13] or from a plot of $\hat{\chi}_\pm$ versus $\hat{\omega}$ curves. The temperature dependence of the spectra is determined by the correlation scale $c_\sigma=|\sigma|^{1/2}$ and by the time scale $t_\sigma=t_0/|\sigma|^{1/2a}$. The scales describe in particular the temperature variation of spectral minima and knees:

$$\omega_k=\hat{\omega}_k/t_\sigma, \quad \omega_{\min}=\hat{\omega}_{\min}/t_\sigma, \quad \chi_k=\hat{\chi}_k c_\sigma,$$
$$\chi_{\min}=\hat{\chi}_{\min}c_\sigma. \tag{3b}$$

The cited results are exact asymptotic formulas for the MCT bifurcation dynamics. Unfortunately, so far no handy formulas for the corrections to the scaling laws are available.

Equations (3) imply some universal features of MCT and most tests of the theory aimed at an assessment of these. For the hard sphere system, all quantities like h_q and λ had been evaluated, and therefore the comparison of MCT predictions and relaxation curves for colloids could be done using the single constant t_0 as fit parameter [4]. For complicated liquids the details of the functional $\mathcal{F}_q$ are not known and, therefore, for example, the comparison of spectra for CKN with Eqs. (3) had to use also h_A and λ as fit parameters [3].

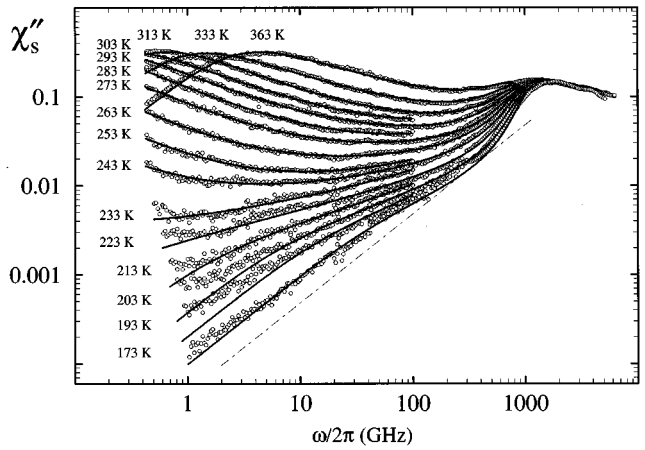

FIG. 1. Susceptibility spectra as measured by Wuttke *et al.* [6] for glycerol by depolarized light scattering (open circles). The experimental data are shown in arbitrary units, and they are normalized so that they coincide for frequencies above 2 THz. Data above 100 GHz are not exhibited for $T=303$, 283, 253, 233, 213, and 193 K in order to avoid overcrowding of the figure. The dashed-dotted straight line indicates a white noise spectrum, $\chi''_{\mathrm{white}}(\omega)\propto\omega$. The full lines are MCT solutions for the model defined by Eqs. (4) with model parameters described in the text.

All systems, which have so far been described successfully by MCT results, are fragile in Angell's classification [14]. Glycerol is between fragile and strong, so that a quantitative test of MCT results against its dynamics is of particular interest.

The various partial structure factors, which quantify the mode-coupling functional $\mathcal{F}_q$, are not available for glycerol at present. Therefore a complete discussion of this system within MCT is not yet possible. To proceed beyond discussing the universal asymptotic results, we will base our calculations on a two-component schematic model. This model is a caricature of the general equations of motion (1) by an $M=2$ specialization. The first correlator $\Phi_1(t)$, to be denoted as $\Phi(t)$, is meant to represent the large set of density fluctuation correlators, which deal with the structure dynamics of glycerol. The second correlator $\Phi_2(t)$, to be denoted as $\Phi_s(t)$, is meant to describe the dynamics of the probing variable A, which is studied in the light scattering experiment. In Sec. II the model will be defined precisely, and its results will be shown to fit the mentioned glycerol light scattering spectra. In Sec. III we will examine how the solutions of the model can be described by the leading order result (3a). Indeed it will be shown that only a part of the measured spectra fall in the range of validity of the scaling law description. In Sec. IV some general conclusions shall be added to the discussion.

II. DATA INTERPRETATION BY A SCHEMATIC MCT MODEL

The following discussion is based on Fig. 1, which exhibits a comparison of MCT solutions for the frequency window 0.4 GHz $\leqslant\omega/2\pi\leqslant$800 GHz with the depolarized light scattering spectra of Wuttke *et al.* [6]. There is no obvious qualitative difference between the glycerol spectra reproduced in Fig. 1 and those discussed by Rössler *et al.* [5] or Sokolov, Steffen, and Rössler [8]. The latter refer to the considerably

smaller window $\omega/2\pi \geqslant 50$ GHz, so that their fit by MCT formulas would be less demanding than the fits shown in this paper. The shown spectra were published [6] in an unnormalized form. We have normalized them so that they agree for frequencies above 2 THz, as reported for the Raman spectra of Ref. [5].

Let us start with a comment on a particular point of concern in Refs. [5–8]. The measured spectra $I(\omega)$, which are related to the susceptibility spectra of Fig. 1 by a trivial frequency factor $I(\omega)\omega \propto \chi''(\omega)$, exhibit a bump at the lower edge of the Raman band. From Fig. 1 of Ref. [6] one infers that the center of the bump is located near 1 THz, and that its low frequency tail influences the spectra down to about $\omega_0/2\pi \approx 400$ GHz. The mentioned bump is referred to [5–8] as the boson peak. It represents oscillatory rather than relaxational motion. For a normal liquid one would expect the spectrum $I(\omega)$ to be essentially frequency independent for $\omega < \omega_0$. Such white noise spectrum is equivalent to a linear variation of the susceptibility spectrum with frequency: $\chi''_{\text{white}}(\omega) \propto \omega$. A white noise line is added in dashed dotted to Fig. 1 as a guide to the eye. Equation (2b) implies that the $\Phi''(\omega) = \chi''(\omega)/\omega$ versus ω curve decreases monotonically for a relaxation process. For a relaxation process the slope of the $\log\chi''$ versus $\log\omega$ diagram must not exceed unity. The bosom peak manifests itself in Fig. 1 by the tendency of the spectrum to increase more steeply than the dashed dotted line with increasing $\log\omega$ for $\omega \geqslant \omega_0$.

One notices that the susceptibility spectra in Fig. 1 for T near 223 or 233 K vary sublinearly, $\chi''(\omega) \propto \omega^a$, $a \approx 0.3$, for the two-decade window $\omega/2\pi < 100$ GHz. The sublinear susceptibility spectra lead to an enhancement of the spectra for $\omega/2\pi \approx 1$ GHz above χ''_{white} by more than one order of magnitude. The neutron scattering cross section [7] exhibits a corresponding enhancement $I(\omega) \approx 1/\omega^{1-a}$ above a frequency-independent background. MCT has predicted the mentioned power law spectrum as the critical spectrum of the relaxation for temperatures near T_c . The critical spectrum was first observed for CKN by neutron [15] and light scattering [16] spectroscopies, respectively. It appears as a remarkable experimental observation that glycerol exhibits the critical spectrum as clearly as the fragile CKN. This fact seems to be a hint that MCT might also be relevant for the discussion of nonfragile systems.

The high frequency wing of the α peak is visible in Fig. 1 for $T \geqslant 243$ K. The crossover from this wing to the normal liquid spectrum for $\omega/2\pi \geqslant 1$ THz produces a susceptibility minimum at some frequency $\omega_{\min}$. Since the α-peak tail is superimposed on the critical spectrum, the intensity $\chi_{\min} = \chi''(\omega_{\min})$ is enhanced by more than a factor 10 above $\chi''_{\text{white}}(\omega_{\min})$. If one tries to fit the spectral minimum by a sum of some standard model for the α spectrum and a vibrational spectrum found from the low temperature spectrum, one misses the measured minimum intensity $\chi_{\min}$ of glycerol by at least one order of magnitude. This fact was explicitly demonstrated before for the CKN data [17]. Wuttke *et al.* [6] have shown that the α-peak wing can be used to estimate a von Schweidler exponent $b \approx 0.6$. This implies $\lambda \approx 0.7$, which in turn leads to $a \approx 0.3$. The α-peak tails are described reasonably by the master function $\hat{\chi}_-$. However, independent of the choice of λ, the light scattering spectra for $T \geqslant 273$ K and

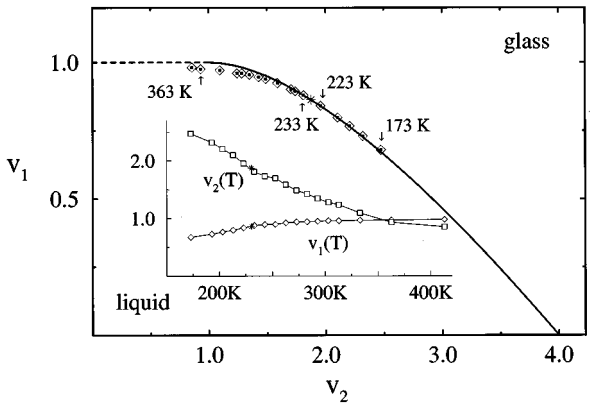

FIG. 2. Coupling constant plane for the model defined by Eqs. (4a) and (4b). The full line is the curve of liquid-to-glass transitions. The diamonds with dots mark the v_1-v_2 pairs, chosen for the solutions of Fig. 1. The inset shows the same parameters v_1 and v_2 as function of temperature, connected by lines as guides to the eye. The stars indicate the transition point for the chosen parameter path $(v_1(T), v_2(T))$.

$\omega > \omega_{\min}$ cannot be described by the leading asymptotic formula (3a) [5,6].

Equation (3a) is reproduced by every MCT example, provided it can reproduce the desired value for λ. The simplest example deals with a single correlator, say $\Phi(t)$, and uses a quadratic polynomial in Eq. (1b). The transient dynamics is specified by some frequency Ω and some damping constant ν. The equation of motion reads

$$\partial_t^2\Phi(t) + \nu\partial_t\Phi(t) + \Omega^2\Phi(t) + \Omega^2\int_0^t m(t-t')\partial_{t'}\Phi(t')dt' = 0. \tag{4a}$$

The mode coupling polynomial is quantified by two coupling constants $v_{1,2} \geqslant 0$,

$$m(t) = v_1\Phi(t) + v_2\Phi(t)^2. \tag{4b}$$

The bifurcations from the weak coupling liquid states to the strong coupling glass states occur at a parabola curve in the $v_1 - v_2$ plane, which is shown as full line in Fig. 2. If v_2 decreases from 4 to 1, the exponent parameter λ increases from $\frac{1}{2}$ to 1 [18]. The model exhibits a number of nongeneric features like the transition singularities along the straight line, which is indicated in Fig. 2 by a dash. These are well understood but they are of no particular interest for the discussion in this paper. The specified model shall be used as a caricature of all the density fluctuations of glycerol. This model represents all the oscillatory modes by a single oscillator. For the probing variable a second correlator, called $\Phi_s(t)$, shall be used. Its equation of motion reads like Eq. (4a) with Φ, Ω, ν, and $m(t)$ replaced by Φ_s , Ω_s , ν_s , and $m_s(t)$, respectively. The kernel $m_s(t)$ shall be specified by a single coupling constant $v_s \geqslant 0$ as the quadratic expression

$$m_s(t) = v_s\Phi(t)\Phi_s(t). \tag{4c}$$

The peculiarity of this model is that the first correlator influences the dynamics of the second, but not vice versa. This

model was introduced by Sjögren [19] as a caricature for the self-motion or tagged particle dynamics of a liquid.

The full lines in Fig. 1 show the susceptibility spectra $\chi_s''(\omega)$ as obtained by solving Eqs. (4a)–(4c). To achieve the intended fits we have chosen temperature-independent values $\Omega/2\pi=16.51$ THz, $\nu=0$, $\Omega_s/2\pi=0.3086$ THz, $\nu_s/2\pi=0.3813$ THz, and $v_s=31.65$. The inset in Fig. 2 shows the drift of the chosen fit parameters v_1 and v_2 as function of temperature. For vanishing v_s, $\chi_s''(\omega)$ would be a damped oscillator spectrum whose low frequency part falls below the dashed dotted line in Fig. 1. Essentially the same would be true if a model with $v_1<0.2$, $v_2<1$ would be considered. The strong spectra shown in Fig. 1, which stretch over a three-decade window and vary with T drastically, result entirely from the smooth drift of the coupling constants (v_1,v_2), which are shown in Fig. 2 by diamonds with dots. The mode-coupling parameters are shifted through the bifurcation line; the intersection point $v_1^c=0.863$, $v_2^c=1.88$, which is indicated in Fig. 2 by a star, leads to an exponent parameter $\lambda=0.730$. This implies the anomalous exponents $a=0.314$ and $b=0.591$. The critical temperature T_c is located between 223 and 233 K.

We anticipate that the shown fits represent an acceptable description of the measured evolution of structural relaxation in glycerol within the GHz band for 173 K $\leqslant T\leqslant$363 K. The fit includes the low frequency wing of the boson peak, and treats the crossover from oscillatory to relaxational dynamics. The results shown suggest the conclusion that the evolution of structural relaxation in glycerol matches the physical picture provided by the MCT [10].

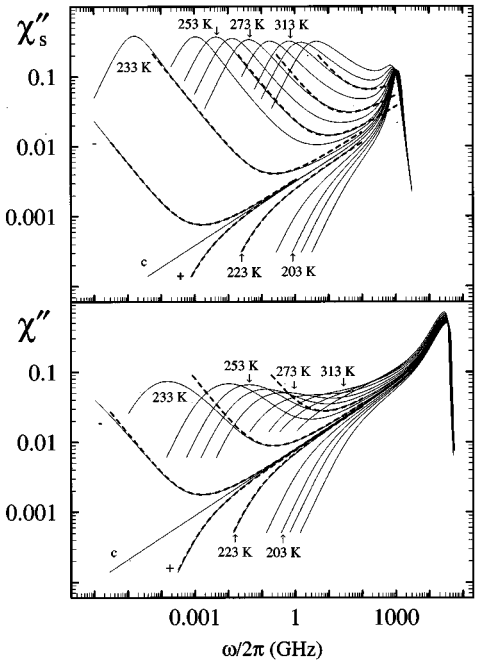

FIG. 3. The solution for χ_s'' from Fig. 1 on an extended abscissa (upper part). The results for 283 and 303 K have not been exhibited in order not to overcrowd the figure. The lower part exhibits the corresponding susceptibility spectra χ'' of the first component Φ of the model. Curves c, $+$, and $-$ denote solutions at the critical point $v_1^c=0.863$, $v_2^c=1.88$, and $v_1=v_1^c\pm 2\times 10^{-5}$ and $v_2=v_2^c$, respectively. The dashed lines exhibit properly shifted master spectra $\hat{\chi}_\pm$, Eq. (3a), for the exponent parameter $\lambda=0.730$.

III. SCALING LAW DESCRIPTION

The evaluated spectra shall be used to discuss quantitatively the connection between the solutions for the specified model and the leading order asymptotic formulas (3). The upper part of Fig. 3 reproduces the MCT results of Fig. 1; the window is enlarged so that the α peaks can be included in the discussion. The lower part exhibits the corresponding results for the other correlator Φ. The spectra at the critical point are added as curves with label c. Two further spectra, labeled $\pm$, are also shown. These are calculated for the two points $v_1=v_1^c\pm 2\times 10^{-5}$ and $v_2=v_2^c$. They correspond to very small separations $|\sigma|$, and the parameters are placed symmetrically with respect to the critical point: $T_\pm=T_c \mp \delta T$, and $\delta T>0$.

Rescaling of the master spectra $\hat{\chi}_\pm$, as described in Eq. (3a) by c_σ and t_σ, is done in the double logarithmic representation of Fig. 3 by parallel shifts of the $\log\hat{\chi}$ versus $\log\omega$ curve. The master spectra for $\lambda=0.730$ are shown as dashed curves. If the minima of $\hat{\chi}_-$ and of the curve labeled by $-$ are placed on top of each other, both spectra for T_+ and T_- are described properly by Eq. (3a) for a large window. Small corrections to the leading order results, Eq. (3a), become visible for χ_s'' for frequencies above 1 GHz and for χ'' for frequencies below 0.01 MHz. The leading corrections to the leading order result for χ_s'', Eq. (3a), increase proportionally to $|\sigma|^{1/2}$, and as a consequence the window of applicability of Eq. (3a) shrinks with increasing $|T-T_c|$. The size of the correction can be different for different correlators. This phenomenon is demonstrated in Fig. 3 for the $T=233$ K curves. The shifted master spectrum $\hat{\chi}_-$ is above the MCT solution $\chi_s''(\omega)$ at 10 GHz, while no discrepancies between the master spectrum and $\chi''(\omega)$ are visible between 0.1 and 100 GHz. The α-peak tail of $\chi_s''(\omega)$ is well described by $\hat{\chi}_-$ down to 0.2 MHz, while $\hat{\chi}_-$ differs from the α-peak tail of $\chi''(\omega)$ already for 20 MHz. If one increases T further, the range of applicability of Eq. (3a) shrinks even more, as is demonstrated for the liquid spectra χ_s'' in Fig. 3 for $T=253$ and 273 K.

The deviation of the shifted $\hat{\chi}_-$ from $\chi_s''(\omega)$ for $\omega>\omega_{\min}$ has a different sign for $T\geqslant 273$ K than for $T=233$ K. This difference cannot be explained by a discussion of the mentioned leading order corrections to Eq. (3a). Rather one has to remember the derivation of the scaling law. This was done via Eq. (2a) for a window, where all transient dynamics could be ignored. It was shown in particular via Eq. (2b) that this window deals with relaxation only. All oscillatory features of the transient dynamics have to be outside the window, where Eqs. (3) can be used. The known general asymptotic MCT formulas cannot be used to discuss glycerol spectra for ω above the identified $\omega_0/2\pi=400$ GHz. For $\omega\geqslant\omega_0$ the boson peak masks the scaling law spectra. This is demonstrated explicitly in Fig. 4 for the $T=253$ K spectrum. The full line reproduces the corresponding fit curve from Fig. 1. The dashed line is the master spectrum $\hat{\chi}_-$ for $\lambda=0.730$. It is shifted so that it can describe well the measured α-peak wing for $\omega/2\pi\leqslant 10$ GHz. Obviously it fits the spectrum around the minimum for a two-and-one-half-

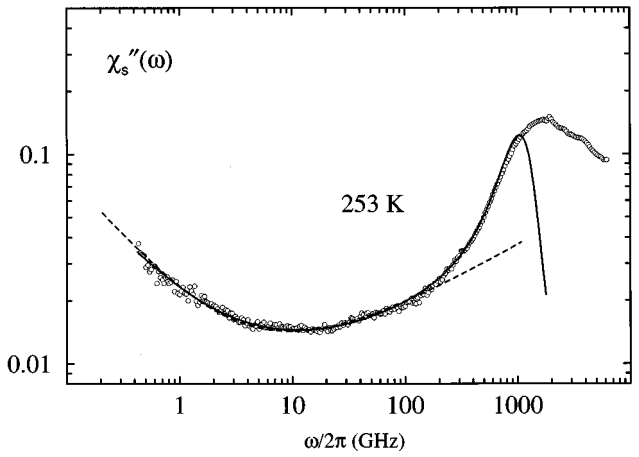

FIG. 4. The MCT spectrum for $T=253$ K from Fig. 1 (full curve) in comparison with the light-scattering spectrum of Wuttke *et al.* [6] (open circles). The dashed line is the scaling law spectrum $\hat{\chi}_-$ for $\lambda=0.730$, rescaled so as to match the α-peak wing of $\omega/2\pi<10$ GHz.

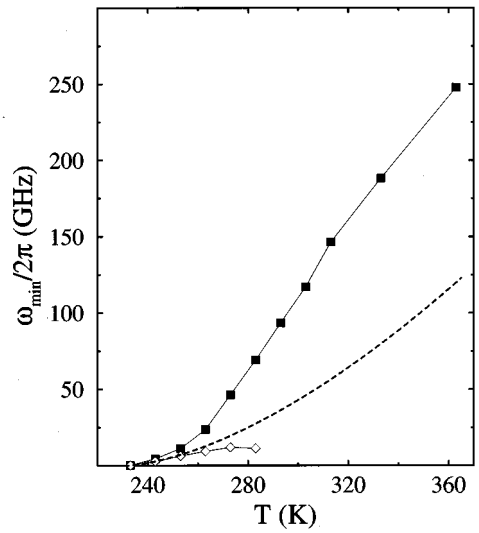

FIG. 5. The position of the susceptibility minima $\omega_{\min}$ for χ_s'' (full squares) and χ'' (open diamonds) obtained from Fig. 3. The lines connecting the symbols are added as guide to the eye. The dashed line is the scaling law asymptote (3b), $\omega_{\min}=C_1(T-T_c)^{1/2a}$, with $1/2a=1.59$, $T_c=230.5$ K, and C_1 chosen to match the minima for 233 K.

decade window. However the critical spectrum, which shows up in the dashed master curve for $\omega/\omega_{\min}\gtrsim 10$, does not describe the MCT results. For $\omega/2\pi>200$ GHz the MCT spectra increase with increasing ω strongly above the relaxation spectrum in agreement with the data. The spectrum for 0.2 THz $\lesssim\omega/2\pi\lesssim$1 THz deals with the crossover from structural relaxation to oscillatory transient motion. Figures 3 and 4 corroborate the conclusion of Ref. [6], that the light scattering spectra within the GHz band can only partly be explained by the scaling laws (3). They confirm also the observation of Refs. [5,8], that the Raman spectra of glycerol, which deal with the dynamics above 50 GHz, cannot be fitted with the leading order asymptotic formulas (3). However, our results, in particular our Figs. 1 and 2, are not in accord with the statements of Sokolov, Steffen, and Rössler [8] that ''strong deviations from MCT predictions have been found for the nonfragile liquid glycerol,'' and that, ''in the nonfragile system glycerol, MCT fails to describe the spectra.''

If the scaling law applies, a spectrum $\chi''(\omega)$ for $T_-=T_c+\delta T$ determines that $T_+=T_c-\delta T$, since $|\sigma(T_+)|=|\sigma(T_-)|$. This is exemplified for the curves $\pm$ in Fig. 3. The spectra for $T<T_c$ exhibit a knee, while those for $T>T_c$ exhibit a minimum, as was explained in Sec. I. The position ω_k of the knee and the corresponding spectral intensity χ_k for $T=T_+$ can be determined via Eq. (3b) from the minimum position $\omega_{\min}$ and minimum intensity $\chi_{\min}$ for $T=T_-$. This result is of potential relevance for the interpretation of spectra. If the spectra of some system for T_+ could be measured for such δT, where the minimum was identified at T_-, one could test the following implications of Eqs. (3b): $\omega_k=\omega_{\min}(\hat{\omega}_k/\hat{\omega}_{\min})$ and $\chi_k=\chi_{\min}(\hat{\chi}_k/\hat{\chi}_{\min})$.

Equation (3a) implies that the position $\omega_{\min}$ is the same for all probing variables A. This implication is obvious in Fig. 3, if one compares the spectral minima of χ_s'' with those of χ'' for $T=T_-$ or for $T=233$ K. In Fig. 5 the minima positions for the two susceptibilities of our model are compared. For $T>260$ K the corrections to the leading order results become so important that the two minima are located at quite different positions. The total intensity of the α peak of the correlator Φ is only 27%. Upon increasing T it becomes buried under the low frequency wing of the microscopic excitation band; for $T\gtrsim 285$ K the susceptibility χ'' no longer exhibits a minimum. The α-peak intensity of χ_s'' is so strong that the spectra show a minimum for all temperatures studied. As explained above, the low frequency wing of the boson peak covers the critical spectrum for $T>270$ K. The minimum of χ_s'' for $T>270$ K is therefore produced by the crossover of the α-peak tail to the boson peak spectrum. This crossover is described by MCT as shown in Fig. 1, but it is outside the range of validity of formulas (3). The variation of the two minima positions with changes of T, described here for the two spectra χ'' and χ_s'', was discussed recently by Toulouse, Pick, and Dreyfus [20] in a comparison of two susceptibility spectra of salol. These authors compared minima positions which were obtained by neutron and light scattering, spectroscopy.

The power laws for the scales, which are obtained by MCT in a leading order asymptotic description for small distances $|T-T_c|$, are identified most clearly by considering a rectification diagram. Since $\omega_{\min}\propto|\sigma|^{1/2a}$, the $\omega_{\min}^{2a}$ versus T graph is proportional to $T-T_c$ within the range of validity of Eqs. (3). Similarly, since the susceptibility maxima follow the power law $\omega_{\max}\propto|\sigma|^{\gamma}$, $\gamma=1/2a+1/2b$, the $\omega_{\max}^{1/\gamma}$ versus T curve also linearly intersects the abscissa at T_c. Figure 6 exhibits the corresponding results obtained from Fig. 3 for $\chi_s''(\omega)$. In agreement with the preceding discussion, one notices that the power laws for the scales are followed for $T<253$ K. A linear extrapolation of the rectified diagrams for $|T-T_c|\leqslant 30$ K therefore yields a reasonable estimation of the critical temperature T_c. The α-peak position is measured by light scattering experiments only for temperatures above 310 K. But for $T>300$ K one is outside the range of validity of Eqs. (3), and therefore the power laws for the scales are no longer valid. If one would extrapolate linearly $1/\tau^{1/\gamma}$ versus

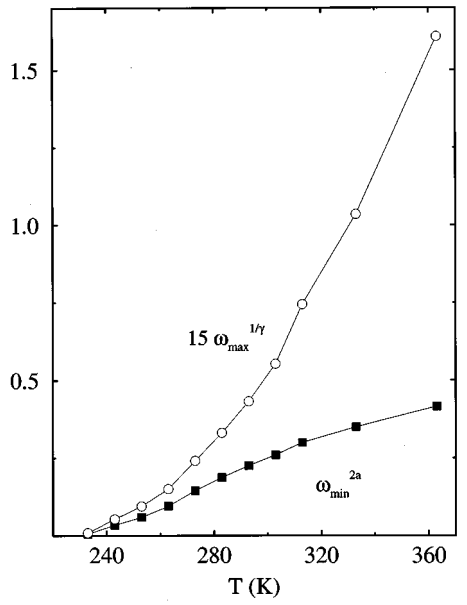

FIG. 6. Minima positions $\omega_{\min}$ (in units of 2π THz) to the power $2a=0.628$ (full squares) and maxima positions $\omega_{\max}$ (in units of 2π THz) to the power $1/\gamma=0.410$ (open circles), as obtained from Fig. 3 for the susceptibility spectra χ_s'', as function of temperature. The lines connecting the symbols are guides to the eye.

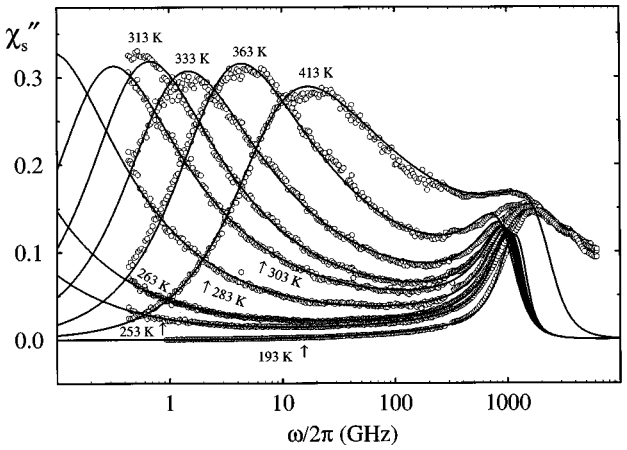

FIG. 7. Some of the data and calculated spectra from Fig. 1 in a semilogarithmic representation. Added are the data for 413 K [6] and a fit by the solution of Eq. (4) with parameters specified in the text.

T curves from $T>300$ K to lower temperatures, one would estimate quite a wrong value for T_c, as is obvious from Fig. 6 for our $1/\tau=\omega_{\max}$ results.

IV. CONCLUSIONS

Some additional remarks shall conclude our discussion. MCT predicts within the leading asymptotic limit that the α-peak shapes are determined by the functional $\mathcal{F}_q$. No generally valid result for the full α-peak shapes can be justified. A discussion of the α-peak shapes for glycerol would require the derivation of $\mathcal{F}_q$ within a microscopic theory and a solution of Eqs. (1) in a similar way as was done earlier for the hard sphere liquid and some other simple liquid models. One could also try to fit the data within more involved schematic models, so that α peaks are described. In any case there is no reason to assume that the α-peak shapes of the schematic model in Fig. 3 have a quantitative relation to the ones for light scattering spectra of glycerol for $\omega/2\pi<0.4$ GHz.

Obviously, there is no possibility to describe the conventional Raman spectrum of glycerol within the full THz window with our two oscillator model. However, in this context it is reassuring that Alba-Simionesco and Krauzman [21] succeeded in fitting complete Raman spectra with a two component MCT model for some glass former. Their fits also describe the evolution of the high frequency part of the structural relaxation. However their results are based on a more involved connection between MCT correlators and Raman response functions than we used here.

One expects that the considered large variation of the temperature also causes some changes of the oscillator parameters Ω, ν, Ω_s, and ν_s. One also expects a temperature drift of the mode coupling coefficient v_s in Eq. (4c) of the same order as considered in Fig. 2 for v_1 and v_2. These drifts have been ignored in our fits for the sake of mathematical simplicity. Thereby we could distinguish between temperature variations of the spectra caused by trivial parameter drifts on the one hand, and the consequences of drifts of the crucial mode coupling parameters near the bifurcation singularity on the other hand. In Ref. [6] one further spectrum was reported for the very high temperature $T=413$ K. It was not possible to fit this spectrum with the mentioned constraint for the model parameters. However, choosing the drifted parameters for the second correlator $v_s=18.8$, $\Omega_s/2\pi=0.7325$ THz, and $\nu_s/2\pi=1.13$ THz (keeping Ω, ν unchanged) the solution for $\chi_s''(\omega)$ also reasonably interpolates these data. This is shown in Fig. 7, where the more conventional semi logarithmic representation of spectra is used.

Let us point out two further implications of the v_1-v_2 drift, which are not directly related to the bifurcation phenomenon. First, the cage effect, as described by the mode coupling functional $\mathcal{F}_q$, leads to a considerable renormalization of the oscillator frequencies. The susceptibility peaks in Fig. 3 are located at higher frequencies than the ''bare'' frequencies Ω_s and Ω, respectively. Second, the high frequency spectra also exhibit characteristic drifts with temperature. These high frequency spectra $\Phi_s''(\omega)$ are exhibited for some representative temperatures in Fig. 8 on linear scales. For such diagrams the boson peak shows up very directly for $T\leqslant 293$ K. The boson peak frequency is found to decrease, and the boson peak intensity is found to increase upon heating. This vibrational softening with increasing temperature can be understood for our model from elementary formulas, which have been obtained by solving Eqs. (4) analytically in the strong coupling limit [18].

There are several experimental techniques yielding correlators as a function of time within the ps window. Therefore it might be worthwhile to show the results for our model in Fig. 9, which underlie the fit curves in Fig. 1. The boson peak of the spectra manifests itself as a pronounced oscillation of Φ_s for times between 0.1 and 1 ps. Figure 1 shows, that our model does not describe properly the smearing of the Raman spectra. The oscillations in Fig. 9 are therefore to some extent an artifact of the applied oversimplifications. If

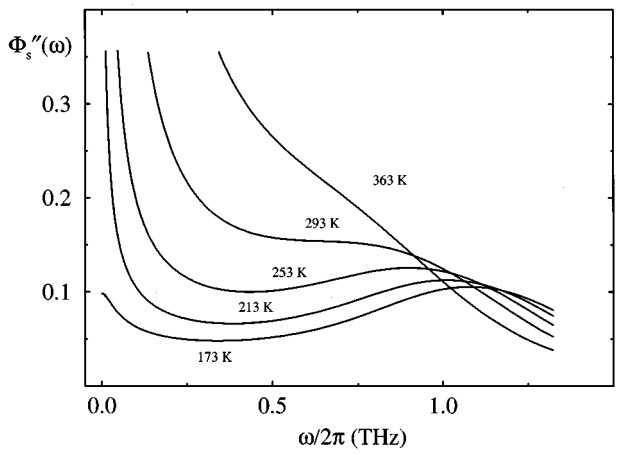

FIG. 8. Relaxation spectra $\Phi_s''(\omega)=\chi_s''/\omega$ in units of $(2\pi$ THz$)^{-1}$ for the MCT solutions shown in Fig. 1 for some representative temperatures.

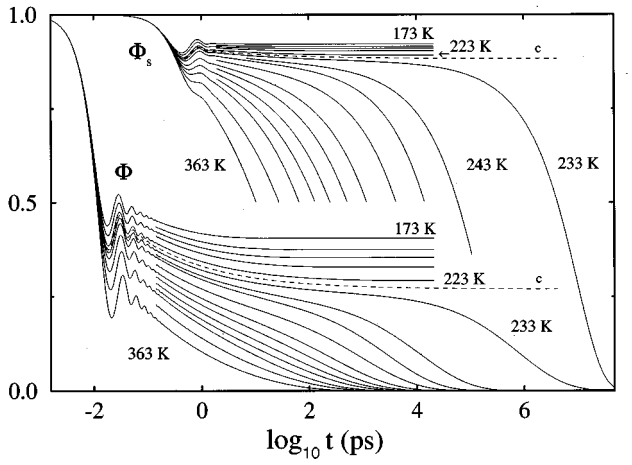

FIG. 9. The solutions $\Phi(t)$ and $\Phi_s(t)$ of Eqs. (4) used to evaluate the spectra in Figs. 1 and 3. The dashed lines with label *c* exhibit the solutions at the transition point.

we would have used a more involved regular kernel $M_s^{\mathrm{reg}}(t)$ in Eq. (1a) so that the Raman band between 1 and 10 THz would be fitted, we would have obtained a transient dynamics with less pronounced oscillations than that shown in Fig. 9. The critical correlators, i.e., the solutions at the critical point, are shown as dashed curves in Fig. 9. They decay toward the critical nonergodicity parameters $f_q^c=f_q(T=T_c)$ which for our model read $f^c=1-\lambda=0.270$ and $f_s^c=1-1/(v_s f^c)=0.883$.

It is well understood that proper extensions of the MCT eliminate the discussed sharp transition to an ideal glass at T_c in favor of some smooth crossover for T near T_c [11]. There is still a regime of parameters and frequencies where Eq. (3a) holds. However, the simple scaling law $\hat{\chi}$ has to be generalized to a two parameter scaling law. The master spectra are still given by λ, but in addition to σ there appears a second relevant control parameter, called the hopping parameter $\delta \geqslant 0$. A first test of the indicated results of the extended MCT against data was done for the mentioned CKN spectra [22]. From this work one infers that some $\delta \neq 0$ effects can also be fitted with a $\delta=0$ theory by erroneously choosing too small a value for λ. We cannot exclude that our analysis suffers from this mistake. The $\log\chi_s''$ versus $\log\omega$ curves for 193 and 203 K in Fig. 1 are somewhat steeper for $\omega/2\pi<8$ GHz than the curves suggested by the data. This systematic discrepancy between data and fit is a signature of $\delta \neq 0$ effects. However, the data studied here do not allow for a meaningful quantitative analysis of δ effects.

Figure 3 shows that important low frequency features of the spectra for $T \leqslant 260$ K fall outside the studied window. Therefore our fits cannot be used as a reliable estimation of λ. Indeed, we have also produced fits of a quality similar to the one shown in Fig. 1 for other parameters λ. We have not systematically examined the possibility for fits of the glycerol spectra for other parameter sets than those mentioned above. Therefore the preceding analysis is not meant to be a determination of MCT parameters for glycerol; rather it is merely offered as a demonstration that relevant spectra for a nonfragile glass former can be interpreted within the MCT, even within a very primitive schematic model. Any further conclusion could be reached only if susceptibility spectra for some probing variable *A* were available, which extend for all cited temperatures from 1 THz down into the middle of the MHz band.

ACKNOWLEDGMENTS

We are very indebted to H. Z. Cummins for many helpful discussions and suggestions. We thank also W. Petry, A. P. Sokolov, and J. Wuttke for comments; and we acknowledge gratefully the permission by the authors of Ref. [6] to use their data files. Our work was supported by Verbundprojekt BMBF 03-G04TUM.

[1] J. Wong and C. A. Angell, *Glass: Structure by Spectroscopy* (Dekker, Basel, 1976).

[2] N. Menon, K. P. O'Brien, P. K. Dixon, L. Wu, S. R. Nagel, B. D. Wiliams, and J. P. Carini, J. Non-Cryst. Solids **141**, 61 (1992); P. Lunkenheimer, A. Pimenov, B. Schiener, R. Böhmer, and A. Loidl, Europhys. Lett. **33**, 611 (1996); P. Lunkenheimer, A. Pimenov, M. Dressel, Yu. G. Goncharov, R. Böhmer, and A. Loidl, Phys. Rev. Lett. **77**, 318 (1996).

[3] G. Li, W. M. Du, X. K. Chen, H. Z. Cummins, and N. J. Tao, Phys. Rev. A **45**, 3867 (1992).

[4] W. van Megen and S. M. Underwood, Phys. Rev. Lett. **70**, 2766 (1993); Phys. Rev. E. **49**, 4206 (1994).

[5] E. Rössler, A. P. Sokolov, A. Kisliuk, and D. Quitman, Phys. Rev. B **49**, 14 967 (1994).

[6] J. Wuttke, J. Hernandez, G. Li, G. Coddens, H. Z. Cummins, F. Fujara, W. Petry, and H. Sillescu, Phys. Rev. Lett. **72**, 3052 (1994).

[7] J. Wuttke, W. Petry, G. Coddens, and F. Fujara, Phys. Rev. E **52**, 4026 (1995).
[8] A. P. Sokolov, W. Steffen, and E. Rössler, Phys. Rev. E **52**, 5105 (1995).
[9] E. Leutheusser, Phys. Rev. A **29**, 2765 (1984); U. Bengtzelius, W. Götze, and A. Sjölander, J. Phys. C **17**, 5915 (1984); S. P. Das, G. F. Mazenko, S. Ramaswamy, and J. J. Toner, Phys. Rev. Lett. **54**, 118 (1985).
[10] S. F. Edwards and P. W. Anderson, J. Phys. F **5**, 965 (1975).
[11] W. Götze and L. Sjögren, Rep. Prog. Phys. **55**, 241 (1992).
[12] W. Götze and L. Sjögren, J. Math. Anal. Appl. **195**, 230 (1995).
[13] W. Götze, J. Phys. Condens. Matter **2**, 8485 (1990).
[14] C. A. Angell, J. Non-Cryst. Solids **131-133**, 13 (1991).
[15] W. Knaak, F. Mezei, and B. Farago, Europhys. Lett. **7**, 529 (1988).
[16] N. J. Tao, G. Li, and H. Z. Cummins, Phys. Rev. Lett. **66**, 1334 (1991).
[17] H. Z. Cummins, G. Li, W. M. Du, J. Hernandez, and N. J. Tao, Transport Theory Stat. Phys. **24**, 981 (1995).
[18] W. Götze, Z. Phys. B **56**, 139 (1984).
[19] L. Sjögren, Phys. Rev. A **33**, 1254 (1986).
[20] J. Toulouse, R. Pick, and C. Dreyfus, in *Disordered Materials and Interfaces*, edited by H. E. Stanley, H. Z. Cummins, D. J. Durian, and D. L. Johnson, MRS Symposia Proceedings No. 407 (Materials Research Society, Pittsburgh, 1996), Vol. 407, p. 161.
[21] C. Alba-Simionesco and M. Krauzman, J. Chem. Phys. **102**, 6574 (1995).
[22] H. Z. Cummins, W. M. Du, M. Fuchs, W. Götze, S. Hildebrand, A. Latz, G. Li, and N. J. Tao, Phys. Rev. E **47**, 4223 (1993).